Chiral phonon mediated high-temperature superconductivity

Yi Gao ,[*] Yang Pan,[*] Jun Zhou ,[†] and Lifa Zhang [‡]
Phonon Engineering Research Center of Jiangsu Province, Center for Quantum Transport and Thermal Energy Science, Institute of Physics Frontiers and Interdisciplinary Sciences, School of Physics and Technology, Nanjing Normal University, Nanjing 210023, China

(Received 27 June 2022; revised 8 May 2023; accepted 3 August 2023; published 14 August 2023)

Breaking down the traditional perception on phonons which are achiral, the existence of a chiral phonon carrying angular momentum provides possible ways to couple electrons, photons, spins, magnons, and excitons, etc. We theoretically proposed an electron-chiral phonon interaction with a two-phonon process, in contrast to a conventional electron-phonon interaction, and a kind of effective Hubbard interaction through exchanging two chiral phonons is proposed. Taking a two-dimensional diatomic honeycomb lattice as an example, we found this repulsive Hubbard interaction mediated by chiral phonons induces unconventional and high-temperature superconductivity. Moreover, the numerical calculations show an inverse isotope effect which is consistent with experimental observations in high-T_c superconductors. Our finding on an electron-chiral phonon and the associated Cooper pair provides a path to understand the high-T_c superconductivity.

DOI: 10.1103/PhysRevB.108.064510

I. INTRODUCTION

The electron-phonon (E-P) interaction plays an important role in conventional superconductivity according to the Bardeen-Cooper-Schrieffer (BCS) theory. However, the effect of the E-P interaction on the transition temperature (T_c) of high-temperature superconductivity is complicated and ambiguous [1]. In BCS theory, Cooper pairs can be formed through exchanging intermediate phonons which leads to an effective attraction between electrons. It was still under debate whether the E-P interaction is adequate to explain high-T_c superconductivity in cuprates because of the peculiar phenomena: a weak or inverse isotope effect; linear electrical resistivity; and a kink in the electronic dispersion relations [2,3]. Other E-P interaction effects such as an unconventional E-P interaction [4], a polaronic effect [1], a nonadiabatic effect [5], spatial charge inhomogeneity [6], and the rapid increase of E-P coupling strength below the critical point in an optimally doped strange metal [7] further complicate the underlying mechanisms. Beside phonons, other bosons such as magnons and plasmons were proposed to be responsible for the formation of Cooper pairs in a doped Mott insulator [8].

A nontrivial chiral phonon effect, which characterizes the phonon angular momentum (PAM) [9], has been theoretically studied by many researchers [10–23] and has been experimentally observed in various materials such as two-dimensional (2D) materials [24], hybrid organic-inorganic perovskites [25], topological insulators [26], ferromagnets [27–29], antiferromagnetic insulators [30], etc. [31–33]. Interestingly, the chiral phonon effect was also observed through the thermal Hall conductivity in the pseudogap phase of cuprates [34]. This finding was attributed to the spin-phonon interaction [27,35]. It is straightforward to speculate that PAM would strongly affect the interplay of the spin, charge, and phonon in high-T_c superconductors and consequently modify the superconducting (SC) phase transition.

PAM is characterized by $\mathbf{L}^{\mathrm{ph}}_{l,s} = \mathbf{u}_{l,s} \times \mathbf{p}_{l,s}$ which describes the rotation of ions around their equilibrium positions [13]. $\mathbf{u}_{l,s}$ and $\mathbf{p}_{l,s}$ are the displacement and momentum of an sth atom in an lth unit cell, respectively. Usually, the overall PAM $\mathbf{L}^{\mathrm{ph}} = \sum_{l,s} \mathbf{L}^{\mathrm{ph}}_{l,s}$ vanishes due to the time-reversal and inversion symmetries. A nonzero $\mathbf{L}^{\mathrm{ph}}$ and the corresponding phonon magnetization can be obtained in a nonequilibrium chiral system where both time-reversal and inversion symmetries are broken [36–38].

In this paper, we consider an electron-chiral phonon (E-CP) interaction in the framework of strong-coupling theory in the Hubbard model [39]. This interaction is nonadiabatic and is beyond the Born-Oppenheimer approximation because $\mathbf{L}^{\mathrm{ph}}_{l,s}$ is a function of both $\mathbf{u}_{l,s}$ and $\mathbf{p}_{l,s}$. Therefore, the electronic motion does not only depend on ion coordination but also depends on momenta. Our calculations reveal the significant contribution of the E-CP interaction to superconductivity. Moreover, the roles of the E-P interaction and E-CP interaction are numerically studied and compared in this work.

II. MODEL

The Hamiltonian consists of four parts, $H = H_0 + H_{ee} + H_{ep} + H_{e-cp}$ where H_0 is the noninteracting part, H_{ee} is the electron-electron interaction, H_{ep} is the conventional E-P interaction, and H_{e-cp} describes the E-CP interaction. $\hbar = 1$ and $k_B = 1$ are chosen for simplicity. We adopt a tight-binding

[*]These authors contributed equally to this work.
[†]zhoujunzhou@njnu.edu.cn
[‡]phyzlf@njnu.edu.cn

model for a 2D diatomic honeycomb lattice, then $H_0 = \sum_{\mathbf{k}\sigma} \psi^\dagger_{\mathbf{k}\sigma} M_\mathbf{k} \psi_{\mathbf{k}\sigma} + \sum_{\mathbf{q}\nu} \omega^\nu_\mathbf{q} a^{\nu\dagger}_\mathbf{q} a^\nu_\mathbf{q}$, where $\psi^\dagger_{\mathbf{k}\sigma} = (c^\dagger_{\mathbf{k}1\sigma}, c^\dagger_{\mathbf{k}2\sigma})$ and $\psi_{\mathbf{k}\sigma} = (c_{\mathbf{k}1\sigma}, c_{\mathbf{k}2\sigma})^T$. $c^\dagger_{\mathbf{k}s\sigma}$ and $c_{\mathbf{k}s\sigma}$ are the creation and annihilation operators of electrons with momentum $\mathbf{k}$ and spin σ ($\sigma = \uparrow, \downarrow$) on sublattice s ($s = 1, 2$),

$$M_\mathbf{k} = \begin{pmatrix} -\mu & \varepsilon_\mathbf{k} \\ \varepsilon^*_\mathbf{k} & -\mu \end{pmatrix}, \tag{1}$$

where $\varepsilon_\mathbf{k} = t[e^{i(\frac{3}{2}k_x + \frac{\sqrt{3}}{2}k_y)} + e^{i\sqrt{3}k_y} + e^{i(\frac{3}{2}k_x + \frac{3\sqrt{3}}{2}k_y)}]$, t is the hopping integral, and the electron wave vector $\mathbf{k} = (k_x, k_y)$. In addition, $a^{\nu\dagger}_\mathbf{q}$ ($a^\nu_\mathbf{q}$) creates (annihilates) a phonon with wave vector $\mathbf{q} = (q_x, q_y)$ and mode ν, while $\omega^\nu_\mathbf{q}$ is the corresponding phonon's dispersion.

The electron-electron interaction is considered as the Hubbard type, which is $H_{ee} = \frac{U}{N} \sum_{\mathbf{k},\mathbf{k}',\mathbf{q},s} c^\dagger_{\mathbf{k}+\mathbf{q}s\uparrow} c^\dagger_{\mathbf{k}'-\mathbf{q}s\downarrow} c_{\mathbf{k}'s\downarrow} c_{\mathbf{k}s\uparrow}$, where N is the number of unit cells and U is the Coulomb interaction. The conventional E-P interaction is $H_{ep} = \frac{\tilde{g}_{ep}}{\sqrt{N}} \sum_{\mathbf{q},\mathbf{k},s,\sigma,\nu} c^\dagger_{\mathbf{k}+\mathbf{q}s\sigma} c_{\mathbf{k}s\sigma} A^\nu_\mathbf{q}$, where $\tilde{g}_{ep} = g_{ep} m^{-1/4}$ is the E-P coupling strength and m is the mass of the atom. Here, $A^\nu_\mathbf{q} = a^\nu_\mathbf{q} + a^{\nu\dagger}_{-\mathbf{q}}$.

We assume that the electron spin ($\mathbf{S}_{l,s}$) feels as a magnetic field induced by local atomic rotation where the magnetic field is proportional to PAM. Then the E-CP interaction is analogous to the form of spin-orbit coupling (SOC) $\eta \mathbf{L}_{l,s} \cdot \mathbf{S}_{l,s}$ [40] where η is the coupling strength. To simplify our calculations, we assume that η is a constant. In the 2D system we studied, both $L^x_{l,s} S^x_{l,s}$ and $L^y_{l,s} S^y_{l,s}$ do not exist. Then the Hamiltonian of the E-CP interaction is written as

$$\begin{aligned} H_{e-cp} &= 2\eta \sum_{l,s} L^z_{l,s} S^z_{l,s} \\ &= -\frac{\sqrt{2}\eta}{N} \sum_{\nu,\nu',\mathbf{q},\mathbf{q}',s} g^{\nu,\nu'}_{\mathbf{q},\mathbf{q}',s} A^\nu_\mathbf{q} B^{\nu'}_{-(\mathbf{q}-\mathbf{q}')} S^{zss}_{\mathbf{q}'}, \end{aligned} \tag{2}$$

where $B^\nu_\mathbf{q} = a^\nu_\mathbf{q} - a^{\nu\dagger}_{-\mathbf{q}}$ and $S^{zss}_\mathbf{q} = \frac{1}{\sqrt{2}} \sum_{\mathbf{k},\sigma} \sigma c^\dagger_{\mathbf{k}+\mathbf{q}s\sigma} c_{\mathbf{k}s\sigma}$. The derivation of H_{e-cp} is given in Appendix A. The matrix element is

$$g^{\nu,\nu'}_{\mathbf{q},\mathbf{q}',s} = \sqrt{\frac{\omega^{\nu'}_{\mathbf{q}-\mathbf{q}'}}{\omega^\nu_\mathbf{q}}} \xi^\dagger_{\mathbf{q}-\mathbf{q}',\nu'}(s) \begin{pmatrix} 0 & -i \\ i & 0 \end{pmatrix} \xi_{\mathbf{q},\nu}(s), \tag{3}$$

where $\xi_{\mathbf{q},\nu}(s)$ is the polarization vector. It satisfies $g^{\nu,\nu'}_{-\mathbf{q},-\mathbf{q}',s} = -g^{\nu,\nu'*}_{\mathbf{q},\mathbf{q}',s}$.

Here, we need to clarify that the terminology of the "chiral phonon" proposed in recent years usually means the phonon components which carry nonzero angular momentum or phonon modes with circular/elliptical polarizations (thus leading to a local magnetic moment that can couple to the electron spin). In contrast, the "normal" or "nonchiral phonons" means phonon components which do not carry angular momentum or phonon modes with linear polarizations. Consequently, we use the term E-CP interaction to describe that the phonon angular momentum can couple to electron spin. On the contrary, for the conventional E-P interaction, it is common sense that neither phonon angular momentum nor electron spins are important.

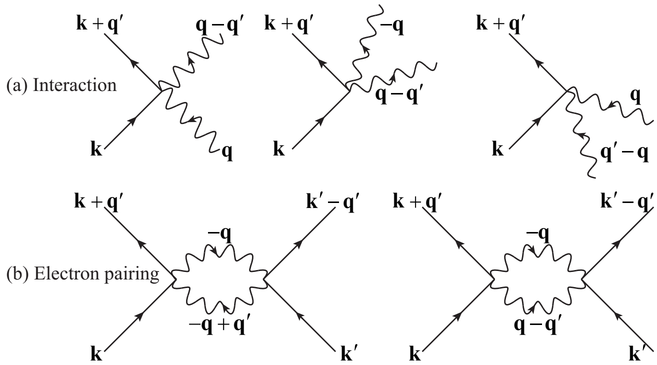

FIG. 1. The Feynman diagrams of the E-CP interaction. (a) Three cases of E-CP interaction for one electron and two phonons. (b) Two cases of electron pairing by exchanging two phonons.

The Feynman diagrams of the E-CP interaction are shown in Fig. 1. The operators in Eq. (2) are $A^\nu_\mathbf{q} B^{\nu'}_{-(\mathbf{q}-\mathbf{q}')}$ which can be expanded as

$$\left(-a^\nu_\mathbf{q} a^{\nu'\dagger}_{\mathbf{q}-\mathbf{q}'} + a^{\nu\dagger}_{-\mathbf{q}} a^{\nu'}_{\mathbf{q}'-\mathbf{q}}\right) - a^{\nu\dagger}_{-\mathbf{q}} a^{\nu'\dagger}_{\mathbf{q}-\mathbf{q}'} + a^\nu_\mathbf{q} a^{\nu'}_{\mathbf{q}'-\mathbf{q}}. \tag{4}$$

So there are three kinds of two-phonon processes in Fig. 1(a): emitting one phonon and absorbing one phonon; emitting two phonons; and absorbing two phonons. Consequently, the second orders of the aforementioned two-phonon processes give rise to two kinds of effective electron-electron interactions as shown in Fig. 1(b). Unlike the BCS theory in which Cooper pairs are formed through exchanging one phonon, the E-CP interaction leads to an effective Hubbard U induced through exchanging two chiral phonons (see Appendix B for details). We must emphasize that the E-CP interaction is fundamentally different from the conventional anharmonic E-P interaction with two-phonon absorption and emission. The chiral phonons are able to affect spin fluctuation and magnetic order which cannot be affected by the anharmonic E-P interaction.

We adopt the widely used Green's function method to investigate the effect of the E-CP interaction on high-T_c superconductivity. First, we calculate the electron's normal Green's function matrix $G(k)$ according to Eq. (1). The matrix elements of the irreducible susceptibility are calculated as [39]

$$\chi_0^{a_1a_4,a_2a_3}(q) = -\frac{T}{N} \sum_k G^{a_2a_4}(k+q) G^{a_1a_3}(k). \tag{5}$$

T is the temperature, and $a_1, a_2, a_3, a_4 = 1, 2$. $G(k) = (ip_n I - M_\mathbf{k})^{-1}$ is the electron's normal Green's function where I is the unit matrix. $q = (\mathbf{q}, i\omega_n)$ and $k = (\mathbf{k}, ip_n)$, where $\omega_n = 2n\pi T$ and $p_n = (2n-1)\pi T$ are the Matsubara frequencies with integer n. Within the random phase approximation (RPA), the spin and charge susceptibilities can be written as [39]

$$\begin{aligned} \chi^{zz}_s(q) &= [I - \chi_0(q)\tilde{S}(q)]^{-1}\chi_0(q), \\ \chi^{+-}_s(q) &= [I - \chi_0(q)U_s]^{-1}\chi_0(q), \\ \chi_c(q) &= [I + \chi_0(q)\tilde{C}(q)]^{-1}\chi_0(q), \end{aligned} \tag{6}$$

where $\chi^{zz}_s(q)$ and $\chi^{+-}_s(q)$ represent the longitudinal and transverse spin susceptibilities, respectively, and $\chi_c(q)$ is the charge susceptibility. The nonzero matrix elements of U_s are $U_s^{a_1a_1,a_1a_1} = U$. In the absence of the E-CP interaction, the nonzero matrix elements of $\tilde{S}(q)$ are $\tilde{S}^{a_1a_1,a_2a_2}(q) = U\delta_{a_1a_2}$. This term can be modified as follows when the E-CP interaction is considered,

$$\tilde{S}^{a_1a_1,a_2a_2}(q) = U\delta_{a_1a_2} - \frac{\eta^2}{N}\sum_{\mathbf{q}_1,\nu_1,\nu_1'} \frac{2(N_1-N_2)(\omega_1-\omega_2)}{(\omega_1-\omega_2)^2+\omega_n^2}\left(g^{\nu_1,\nu_1'}_{\mathbf{q}_1,-\mathbf{q},a_1}g^{\nu_1',\nu_1}_{\mathbf{q}_1+\mathbf{q},\mathbf{q},a_2} + g^{\nu_1',\nu_1*}_{\mathbf{q}_1+\mathbf{q},\mathbf{q},a_1}g^{\nu_1,\nu_1'*}_{\mathbf{q}_1,-\mathbf{q},a_2} + 2g^{\nu_1,\nu_1'}_{\mathbf{q}_1,-\mathbf{q},a_1}g^{\nu_1,\nu_1'*}_{\mathbf{q}_1,-\mathbf{q},a_2}\right)$$
$$- \frac{\eta^2}{N}\sum_{\mathbf{q}_1,\nu_1,\nu_1'} \frac{2(N_1+N_2+1)(\omega_1+\omega_2)}{(\omega_1+\omega_2)^2+\omega_n^2}\left(g^{\nu_1,\nu_1'}_{\mathbf{q}_1,-\mathbf{q},a_1}g^{\nu_1',\nu_1}_{\mathbf{q}_1+\mathbf{q},\mathbf{q},a_2} + g^{\nu_1',\nu_1*}_{\mathbf{q}_1+\mathbf{q},\mathbf{q},a_1}g^{\nu_1,\nu_1'*}_{\mathbf{q}_1,-\mathbf{q},a_2} - 2g^{\nu_1,\nu_1'}_{\mathbf{q}_1,-\mathbf{q},a_1}g^{\nu_1,\nu_1'*}_{\mathbf{q}_1,-\mathbf{q},a_2}\right), \quad (7)$$

where $\omega_1 = \omega^{\nu_1}_{\mathbf{q}_1}$, $\omega_2 = \omega^{\nu_1'}_{\mathbf{q}_1+\mathbf{q}}$ are the phonon dispersion relations and $N_1 = \frac{1}{e^{\omega_1/T}-1}$, $N_2 = \frac{1}{e^{\omega_2/T}-1}$ are the Bose distribution functions.

Finally, the nonzero matrix elements of $\tilde{C}(q)$ are

$$\tilde{C}^{a_1a_1,a_2a_2}(q) = U\delta_{a_1a_2} - 4\tilde{g}_{ep}^2\sum_{\nu}\frac{\omega^{\nu}_{\mathbf{q}}}{\omega^{\nu 2}_{\mathbf{q}}+\omega_n^2}. \quad (8)$$

When temperature is close to T_c, the linearized Eliashberg equation is [39]

$$\lambda\phi^{a_6a_5}(k) = -\frac{T}{N}\sum_q\sum_{a_1,a_2,a_3,a_4} G^{a_1a_2}(k-q)G^{a_4a_3}(q-k) \times \phi^{a_2a_3}(k-q)V^{a_4a_5,a_1a_6}(q), \quad (9)$$

where $\phi(k)$ is the electron's anomalous self-energy. T_c is reached when the largest eigenvalue λ in Eq. (9) reaches 1. The singlet pairing interaction in Eq. (9) is [39]

$$V(q) = \tfrac{1}{2}\tilde{S}(q)\chi_s^{zz}(q)\tilde{S}(q) + U_s\chi_s^{+-}(q)U_s - \tfrac{1}{2}\tilde{C}(q)\chi_c(q)\tilde{C}(q) + \tfrac{1}{2}[\tilde{S}(q)+\tilde{C}(q)]. \quad (10)$$

We set $U = 2.3t$ and adjust the chemical potential μ to ensure the electron filling $n_f = 0.95$ where $n_f = 1 + TN^{-1}\sum_{a_1}\sum_k G^{a_1a_1}(k)$ [corresponding to $\mu \approx -0.485t$ in Eq. (1)]. The Fermi surface and band structure are shown in Figs. 2(a) and 2(b), respectively. The bandwidth is about $6t$, therefore this choice of U corresponds to an intermediate strength of the electron-electron interaction. Since the band structure has particle-hole symmetry, we consider only the hole-doped case and the choice of n_f corresponds to 5% hole doping. $N = 32 \times 32$ and 16 384 Matsubara frequencies are used. The summation over momentum and frequency are both done by fast Fourier transformation. $g^{\nu,\nu'}_{\mathbf{q},\mathbf{q}',s}$ is calculated by given values of m_1 and m_2 which are the masses of two atoms, respectively. When $m_1 = m_2 = 1$, we rescale the phonon's dispersion so the maximal $\omega^{\nu}_{\mathbf{q}} \approx 0.097t$. In this case, the phonon's dispersion can be seen in Fig. 3. The exact calculation of the E-CP coupling strength η is not easy. We speculate that the E-CP interaction is similar to SOC by simply considering an ion rotating around an electron [40]. Then η must decrease with increasing temperature because of the enlarged distance between the electron and ion. Therefore, we assume a simple exponential decay of η as follows,

$$\eta = \eta_0 e^{-T/T^*}. \quad (11)$$

Here, we set $\eta_0 = 4.6574 \times 10^{-4}t$ and $T^* = 0.02t$.

III. RESULTS AND DISCUSSIONS

Starting from $n_f = 0.95$, we calculate the largest eigenvalue of $\chi_0(\mathbf{q}, i\omega_n = 0)\tilde{S}(\mathbf{q}, i\omega_n = 0)$ over all $\mathbf{q}$ and denote it as α_s^{zz}. Its value has to be less than 1 to prevent the formation of static magnetic order. We further denote α_s^{+-} and α_c as the largest eigenvalues of $\chi_0(\mathbf{q}, i\omega_n = 0)U_s$ and $-\chi_0(\mathbf{q}, i\omega_n = 0)\tilde{C}(\mathbf{q}, i\omega_n = 0)$, respectively. Similarly, they have to be less than 1 to stay away from static magnetic and charge ordering.

In the absence of E-CP and E-P couplings, i.e., $\eta = \tilde{g}_{ep} = 0$, we show the evolution of α_s^{zz}, α_s^{+-}, and α_c with temperature in solid curves in Fig. 4(a). It is obvious that $\alpha_s^{zz} = \alpha_s^{+-}$. Through the temperature range we investigated, α_s^{zz}, α_s^{+-}, and α_c are always less than 1. Figure 4(b) shows the largest eigenvalue of Eq. (9), λ, as a function of T. λ increases with

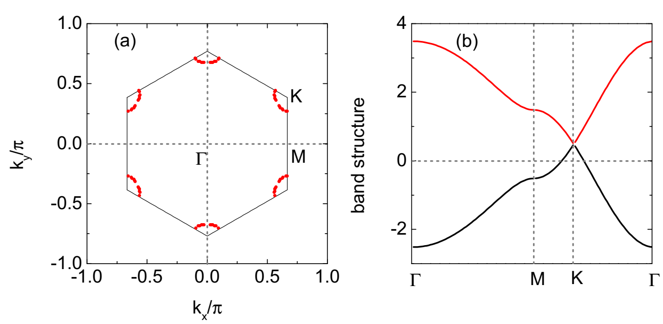

FIG. 2. (a) The Fermi surface in the first Brillouin zone. (b) The band structure along high-symmetry directions. The gray dashed horizontal line in (b) denotes the position of the Fermi level.

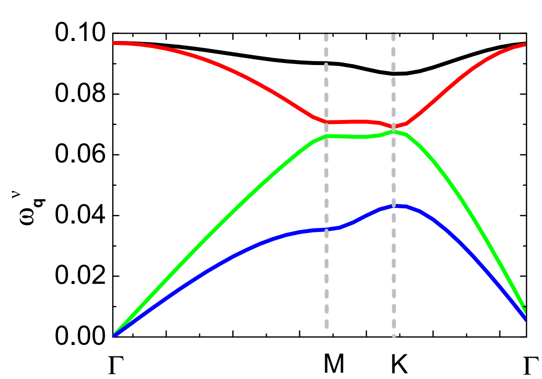

FIG. 3. The phonon's dispersion at $m_1 = m_2 = 1$.

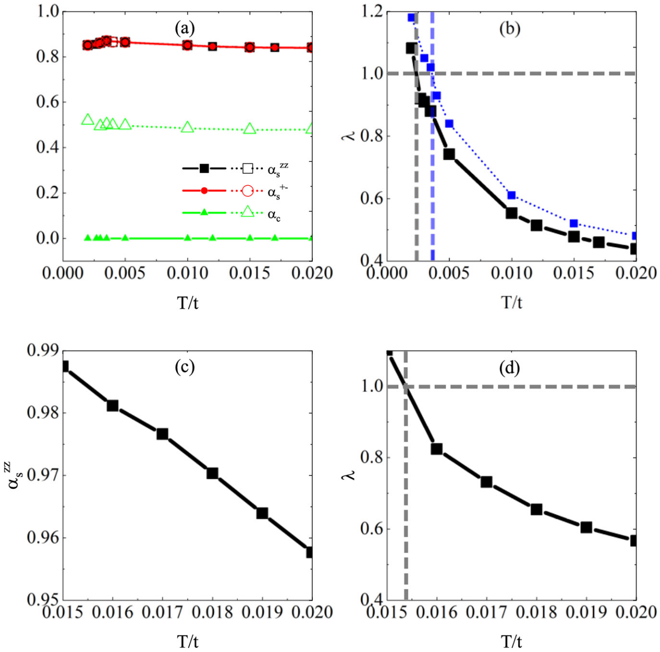

FIG. 4. (a) The evolution of α_s^{zz}, α_s^{+-}, and α_c with temperature when $\eta = \tilde{g}_{ep} = 0$ (solid curves) and $\eta = 0$, $\tilde{g}_{ep} = 0.15t$ (dotted curves). (b) λ as a function of T at $\eta = \tilde{g}_{ep} = 0$ (solid curve) and $\eta = 0$, $\tilde{g}_{ep} = 0.15t$ (dotted curves). (c) The evolution of α_s^{zz} and (d) the evaluation of λ with temperature when η is set according to Eq. (11) and $\tilde{g}_{ep} = 0$. The vertical dashed lines in (b) and (d) denote the value of T when $\lambda = 1$. $U = 2.3t$ is used in all the calculations.

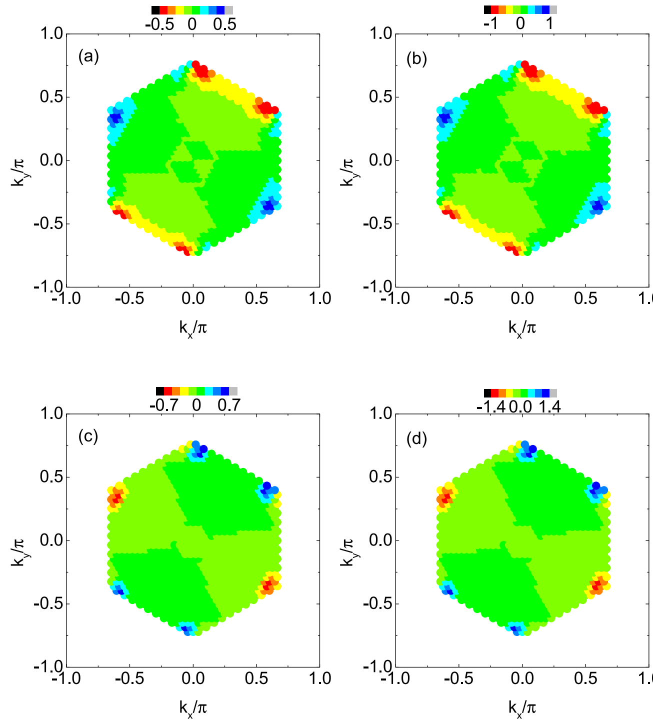

FIG. 5. The calculated (a) real part $\mathrm{Re}\,\Delta^{11}(\mathbf{k}, i\pi T)$ and (b) imaginary part $\mathrm{Im}\,\Delta^{11}(\mathbf{k}, i\pi T)$ of pairing function $\Delta^{11}(\mathbf{k}, i\pi T)$ in the Brillouin zone when $\eta = \tilde{g}_{ep} = 0$ and $T = 0.002t$. (c) and (d) are similar to (a) and (b), respectively, but at $\eta \neq 0$, $\tilde{g}_{ep} = 0$, and $T = 0.015t$.

decreasing T and reaches 1 at $T \approx 0.0025t$, suggesting that $T_c \approx 0.0025t$ when there is neither an E-CP nor E-P interaction. If the E-P coupling is present, for example, $\eta = 0$ and $\tilde{g}_{ep} = 0.15t$, the dotted curves in Figs. 4(a) and 4(b) show that α_c and T_c increase to 0.5 and $0.0035t$, respectively. The spin susceptibility related α_s^{zz} and α_s^{+-} are unaffected by the E-P interaction.

In the presence of the E-CP interaction (but no E-P interaction), the evolution of α_s^{zz} and λ with temperature are shown in Figs. 4(c) and 4(d), respectively. Both α_s^{zz} and λ increase with decreasing temperature, suggesting the trend to have a magnetic phase transition and superconductivity phase transition. However, since when T decreases, λ reaches 1 before α_s^{zz} does, thus the superconductivity phase transition actually occurs and the corresponding $T_c \approx 0.0155t$ as indicated by the vertical dashed line in Fig. 4(d). Therefore, the E-CP coupling can greatly enhance T_c. Moreover, α_s^{+-} and α_c are not shown because only the z component is considered in Eq. (2), so then both of them stay unchanged as shown in Fig. 4(a). Our numerical calculations further confirm that the E-P interaction, by setting $\tilde{g}_{ep} = 0.15t$ in this case, hardly changes the value of T_c. This proves that the great enhancement of T_c is indeed resulting from the E-CP interaction.

The above finding reveals that the E-CP interaction leads to an unambiguous increase of α_s^{zz}. This is because the last two terms in Eq. (7) are positive when $a_1 = a_2$ and negligibly small when $a_1 \neq a_2$. Therefore the phonon can effectively increase the value of U for the longitudinal spin susceptibility, leading to an increased α_s^{zz}, which means an increased longitudinal spin fluctuation. It enhances the term $\frac{1}{2}\tilde{S}(q)\chi_s^{zz}(q)\tilde{S}(q)$ in Eq. (10), leading to an enlarged pairing interaction, which then results in an enhanced T_c.

We now turn to investigate the pairing symmetry by projecting $\phi(k)$ in Eq. (9) onto each band. We only consider the pairing function on the lowest band $[\Delta^{11}(k)]$, which crosses the Fermi level. When $\eta = \tilde{g}_{ep} = 0$, the superconductivity pairing results solely from the electron-electron interaction. In this case, at T $(0.002t)$ slightly below T_c $(0.0025t)$, we show the real and imaginary parts of $\Delta^{11}(\mathbf{k}, i\pi T)$ in Figs. 5(a) and 5(b), respectively. One can see that $\mathrm{Re}\,\Delta^{11}(\mathbf{k}, i\pi T)$ and $\mathrm{Im}\,\Delta^{11}(\mathbf{k}, i\pi T)$ differ only in magnitude, but have the same structure in momentum space. Therefore the phase factor between the real and imaginary parts is global and $\Delta^{11}(\mathbf{k}, i\pi T)$ can be taken as real, i.e., no time-reversal symmetry breaking. Furthermore, there exist sign changes in $\Delta^{11}(\mathbf{k}, i\pi T)$, indicating that the pairing symmetry is unconventional (not isotropic s wave). When $\eta \neq 0$ and $\tilde{g}_{ep} = 0$, the pairing function at $0.015t < T_c = 0.0155t$ shown in Figs. 5(c) and 5(d) remains qualitatively the same as that for $\eta = 0$. The pairing still does not break the time-reversal symmetry and is unconventional as well. We found that the last two terms in Eq. (7) are slightly $\mathbf{q}$ dependent, therefore the E-CP coupling will not vary the pairing symmetry significantly as compared to the $\eta = 0$ case. We have also verified that, in the above two cases, including the E-P interaction at $\tilde{g}_{ep} = 0.15t$ does not change the pairing function qualitatively.

Thus, by introducing the E-CP interaction, high-temperature and unconventional superconductivity can be

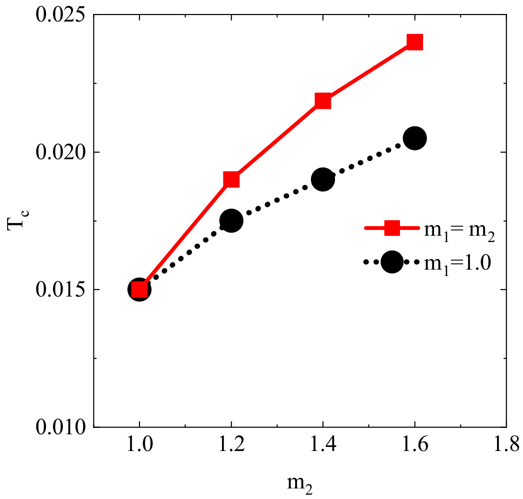

FIG. 6. The isotope effect of T_c. The calculated values of T_c vs m_2 when $m_1 = m_2 = m$ (red) and $m_1 = 1$ (black). Here, $\tilde{g}_{ep} = 0$.

induced in systems with a relatively weak electron-electron interaction. For the present system, taking $t = 1$ eV, the calculated T_c can be boosted from 2.5 meV (29 K) to 15.5 meV (180 K). Furthermore, if the phonon couples to S^x and S^y components of electrons, T_c may be further enhanced since the factor is 1 in the $U_s\chi_s^{+-}(q)U_s$ term in Eq. (10), instead of $\frac{1}{2}$ in the $\tilde{S}(q)\chi_s^{zz}(q)\tilde{S}(q)$ term.

The anomalous isotope effect has been found in many superconductors [41–44]. The E-CP interaction provides an alternative explanation of such isotope effect. First, we consider the case with $m_1 = m_2 = m$. Figure 6 shows that T_c increases with increasing m. Such an inverse isotope effect is opposite to the conventional E-P coupling in BCS theory where T_c decreases with increasing m, because the most significant term, the $\omega_n = 0$ component in Eq. (7), can be written as

$$\begin{aligned}&\tilde{S}^{a_1a_1,a_2a_2}(\mathbf{q}, i\omega_n = 0, m, T)\\&\quad = \sqrt{m}\tilde{S}^{a_1a_1,a_2a_2}(\mathbf{q}, i\omega_n = 0, 1, \sqrt{m}T),\end{aligned} \tag{12}$$

when the phonon dispersion $\sim 1/\sqrt{m}$ and $U = 0$. The matrix elements of $\tilde{S}(q)$ are enhanced as m increases, leading to an inverse isotope effect. The derivation of Eq. (12) is as follows. At $U = 0$ and $\omega_n = 0$, we have

$$\begin{aligned}\tilde{S}^{a_1a_1,a_2a_2}(q) = &-\frac{\eta^2}{N}\sum_{\mathbf{q}_1,\nu_1,\nu_1'}\frac{2(N_1-N_2)}{\omega_1-\omega_2}\left(g^{\nu_1,\nu_1'}_{\mathbf{q}_1,-\mathbf{q},a_1}g^{\nu_1',\nu_1}_{\mathbf{q}_1+\mathbf{q},\mathbf{q},a_2}+g^{\nu_1',\nu_1*}_{\mathbf{q}_1+\mathbf{q},\mathbf{q},a_1}g^{\nu_1,\nu_1'*}_{\mathbf{q}_1,-\mathbf{q},a_2}+2g^{\nu_1,\nu_1'}_{\mathbf{q}_1,-\mathbf{q},a_1}g^{\nu_1,\nu_1'*}_{\mathbf{q}_1,-\mathbf{q},a_2}\right)\\&-\frac{\eta^2}{N}\sum_{\mathbf{q}_1,\nu_1,\nu_1'}\frac{2(N_1+N_2+1)}{\omega_1+\omega_2}\left(g^{\nu_1,\nu_1'}_{\mathbf{q}_1,-\mathbf{q},a_1}g^{\nu_1',\nu_1}_{\mathbf{q}_1+\mathbf{q},\mathbf{q},a_2}+g^{\nu_1',\nu_1*}_{\mathbf{q}_1+\mathbf{q},\mathbf{q},a_1}g^{\nu_1,\nu_1'*}_{\mathbf{q}_1,-\mathbf{q},a_2}-2g^{\nu_1,\nu_1'}_{\mathbf{q}_1,-\mathbf{q},a_1}g^{\nu_1,\nu_1'*}_{\mathbf{q}_1,-\mathbf{q},a_2}\right).\end{aligned} \tag{13}$$

When the masses of the two sublattices are equal ($m_1 = m_2 = m$), and if we define ω_1 and ω_2 as the phonon dispersion relations at $m = 1$, while ω_1' and ω_2' are the phonon dispersion relations at $m \neq 1$, then we will have

$$\begin{aligned}\omega_1' &= \omega_1/\sqrt{m},\\ \omega_2' &= \omega_2/\sqrt{m}.\end{aligned} \tag{14}$$

Similarly, if we define N_1 and N_2 as the Bose distribution functions at $m = 1$, while N_1' and N_2' are the Bose distribution functions at $m \neq 1$, then we will have

$$\begin{aligned}N_1'(T) &= \frac{1}{e^{\frac{\omega_1'}{T}}-1} = \frac{1}{e^{\frac{\omega_1}{\sqrt{m}T}}-1} = N_1(\sqrt{m}T),\\ N_2'(T) &= N_2(\sqrt{m}T).\end{aligned} \tag{15}$$

Finally, if we define $\tilde{S}^{a_1a_1,a_2a_2}(\mathbf{q}, i\omega_n = 0, T)$ as the value of Eq. (13) at $m = 1$ and $\tilde{S}'^{a_1a_1,a_2a_2}(\mathbf{q}, i\omega_n = 0, T)$ at $m \neq 1$, then we will have

$$\begin{aligned}&\tilde{S}'^{a_1a_1,a_2a_2}(\mathbf{q}, i\omega_n = 0, T)\\&= -\frac{\eta^2}{N}\sum_{\mathbf{q}_1,\nu_1,\nu_1'}\frac{2[N_1'(T)-N_2'(T)]}{\omega_1'-\omega_2'}\left(g^{\nu_1,\nu_1'}_{\mathbf{q}_1,-\mathbf{q},a_1}g^{\nu_1',\nu_1}_{\mathbf{q}_1+\mathbf{q},\mathbf{q},a_2}+g^{\nu_1',\nu_1*}_{\mathbf{q}_1+\mathbf{q},\mathbf{q},a_1}g^{\nu_1,\nu_1'*}_{\mathbf{q}_1,-\mathbf{q},a_2}+2g^{\nu_1,\nu_1'}_{\mathbf{q}_1,-\mathbf{q},a_1}g^{\nu_1,\nu_1'*}_{\mathbf{q}_1,-\mathbf{q},a_2}\right)\\&\quad-\frac{\eta^2}{N}\sum_{\mathbf{q}_1,\nu_1,\nu_1'}\frac{2[N_1'(T)+N_2'(T)+1]}{\omega_1'+\omega_2'}\left(g^{\nu_1,\nu_1'}_{\mathbf{q}_1,-\mathbf{q},a_1}g^{\nu_1',\nu_1}_{\mathbf{q}_1+\mathbf{q},\mathbf{q},a_2}+g^{\nu_1',\nu_1*}_{\mathbf{q}_1+\mathbf{q},\mathbf{q},a_1}g^{\nu_1,\nu_1'*}_{\mathbf{q}_1,-\mathbf{q},a_2}-2g^{\nu_1,\nu_1'}_{\mathbf{q}_1,-\mathbf{q},a_1}g^{\nu_1,\nu_1'*}_{\mathbf{q}_1,-\mathbf{q},a_2}\right),\\&= -\sqrt{m}\frac{\eta^2}{N}\sum_{\mathbf{q}_1,\nu_1,\nu_1'}\frac{2[N_1(\sqrt{m}T)-N_2(\sqrt{m}T)]}{\omega_1-\omega_2}\left(g^{\nu_1,\nu_1'}_{\mathbf{q}_1,-\mathbf{q},a_1}g^{\nu_1',\nu_1}_{\mathbf{q}_1+\mathbf{q},\mathbf{q},a_2}+g^{\nu_1',\nu_1*}_{\mathbf{q}_1+\mathbf{q},\mathbf{q},a_1}g^{\nu_1,\nu_1'*}_{\mathbf{q}_1,-\mathbf{q},a_2}+2g^{\nu_1,\nu_1'}_{\mathbf{q}_1,-\mathbf{q},a_1}g^{\nu_1,\nu_1'*}_{\mathbf{q}_1,-\mathbf{q},a_2}\right)\\&\quad-\sqrt{m}\frac{\eta^2}{N}\sum_{\mathbf{q}_1,\nu_1,\nu_1'}\frac{2[N_1(\sqrt{m}T)+N_2(\sqrt{m}T)+1]}{\omega_1+\omega_2}\left(g^{\nu_1,\nu_1'}_{\mathbf{q}_1,-\mathbf{q},a_1}g^{\nu_1',\nu_1}_{\mathbf{q}_1+\mathbf{q},\mathbf{q},a_2}+g^{\nu_1',\nu_1*}_{\mathbf{q}_1+\mathbf{q},\mathbf{q},a_1}g^{\nu_1,\nu_1'*}_{\mathbf{q}_1,-\mathbf{q},a_2}-2g^{\nu_1,\nu_1'}_{\mathbf{q}_1,-\mathbf{q},a_1}g^{\nu_1,\nu_1'*}_{\mathbf{q}_1,-\mathbf{q},a_2}\right),\\&= \sqrt{m}\tilde{S}^{a_1a_1,a_2a_2}(\mathbf{q}, i\omega_n = 0, \sqrt{m}T).\end{aligned} \tag{16}$$

Therefore, increasing m will enhance $\tilde{S}(q)$, leading to an enlarged pairing interaction, thus an enlarged T_c.

In contrast, for the E-P coupling,

$$\tilde{C}^{a_1a_1,a_2a_2}(q) = -\frac{4g_{ep}^2}{\sqrt{m}}\sum_{\nu}\frac{\omega_{\mathbf{q}}^{\nu}}{\omega_{\mathbf{q}}^{\nu 2}+\omega_n^2}. \tag{17}$$

At $\omega_n = 0$, we define

$$\frac{4g_{ep}^2}{\sqrt{m}}\frac{\omega_{\mathbf{q}}^{\nu}}{\omega_{\mathbf{q}}^{\nu 2}+\omega_n^2} = \frac{4g_{ep}^2}{\sqrt{m}}\frac{1}{\omega_{\mathbf{q}}^{\nu}} = \lambda_{\mathbf{q}}^{\nu}, \tag{18}$$

where $\lambda_{\mathbf{q}}^{\nu}$ is independent of m since $\omega_{\mathbf{q}}^{\nu}$ scales as $\frac{1}{\sqrt{m}}$ and it cancels the $\sqrt{m}$ term in the denominator of Eq. (18). Then we have

$$\begin{aligned}\tilde{C}^{a_1a_1,a_2a_2}(q) &= -\frac{4g_{ep}^2}{\sqrt{m}}\sum_{\nu}\frac{\omega_{\mathbf{q}}^{\nu}}{\omega_{\mathbf{q}}^{\nu 2}+\omega_n^2}\\ &= -\sum_{\nu}\frac{4g_{ep}^2}{\sqrt{m}}\frac{1}{\omega_{\mathbf{q}}^{\nu}}\frac{1}{1+\left(\frac{\omega_n}{\omega_{\mathbf{q}}^{\nu}}\right)^2}\\ &= -\sum_{\nu}\frac{\lambda_{\mathbf{q}}^{\nu}}{1+\left(\frac{2n\pi T}{\omega_{\mathbf{q}}^{\nu}}\right)^2}.\end{aligned} \tag{19}$$

It is this relation that produces the normal isotope effect, since $\omega_{\mathbf{q}}^{\nu}(m) = \frac{1}{\sqrt{m}}\omega_{\mathbf{q}}^{\nu}(0)$, therefore $T_c(m) = \frac{1}{\sqrt{m}}T_c(0)$. It should be pointed out that the above normal isotope effect holds because $\lambda_{\mathbf{q}}^{\nu}$ is independent of m, otherwise it will break down, just as our E-CP case.

Compared to the E-P case, besides scaling the temperature T to $\sqrt{m}T$, there is an additional $\sqrt{m}$ term as seen from Eq. (16) in the E-CP case. Therefore the isotope effects are different between the E-P and E-CP cases. The latter has the inverse isotope effect.

In addition, we also investigate the isotope substitution effect in Fig. 6 where $m_1 = 1$ and m_2 changes from 1 to 1.6. We find that T_c also increases with increasing m_2 although the increasing rate is smaller than the previous case. This finding provides a possible explanation of the inverse isotope effect observed in cuprates with an oxygen isotope substitution ($O^{16} \rightarrow O^{18}$) [42,45].

IV. CONCLUSIONS

In summary, we introduce the electron-chiral phonon interaction into the current theory of high-T_c superconductivity. This interaction leads to an interplay of electron, spin, and charge in superconductors. The numerical calculation results show a remarkable enhancement of T_c induced by this interaction. Moreover, both unconventional pairing and a peculiar inverse isotope effect are found which are able to explain the experimental observations. In contrast, our calculation shows that the influence of a conventional electron-phonon interaction is marginal.

ACKNOWLEDGMENTS

J.Z. thanks Prof. Xiangfan Xu for discussions. This work was supported by the National Natural Science Foundation of China No. 11890703 and by Department of Science and Technology of Jiangsu Province (No. BK20220032). J.Z. is thankful for the support from "Shuangchuang" Doctor program of Jiangsu Province (JSSCBS20210341).

APPENDIX A: THE E-CP INTERACTION HAMILTONIAN

The $\mathbf{u}_{l,s}$, $\mathbf{p}_{l,s}$, and $\mathbf{S}_{l,s}^z$ can be written in the second quantization representation

$$\mathbf{u}_{l,s} = \sum_{\mathbf{q},\nu}\sqrt{\frac{1}{2m_sN\omega_{\mathbf{q}}^{\nu}}}\xi_{\mathbf{q},\nu}(s)\big(a_{\mathbf{q}}^{\nu}+a_{-\mathbf{q}}^{\nu\dagger}\big)e^{i\,\mathbf{q}\cdot\mathbf{R}_l}, \tag{A1}$$

$$\mathbf{p}_{l,s} = \sum_{\mathbf{q},\nu}\sqrt{\frac{m_s\omega_{\mathbf{q}}^{\nu}}{2N}}i\xi_{\mathbf{q},\nu}^{*}(s)\big(a_{\mathbf{q}}^{\nu\dagger}-a_{-\mathbf{q}}^{\nu}\big)e^{-i\,\mathbf{q}\cdot\mathbf{R}_l}, \tag{A2}$$

$$\mathbf{S}_{l,s}^z = \sum_{\sigma}\sigma c_{l,s,\sigma}^{\dagger}c_{l,s,\sigma} = \frac{1}{N}\sum_{\mathbf{k},\mathbf{k}',\sigma}\sigma c_{\mathbf{k}',s,\sigma}^{\dagger}c_{\mathbf{k},s,\sigma} * e^{i\,(\mathbf{k}-\mathbf{k}')\cdot\mathbf{R}_l}. \tag{A3}$$

The H_{e-cp} is

$$\begin{aligned}H_{e-cp} &= 2\eta\sum_{l,s}L_{l,s}^zS_{l,s}^z\\ &= 2\eta\sum_{l,s,\sigma}\big(u_{l,s}^xp_{l,s}^y-u_{l,s}^yp_{l,s}^x\big)\sigma c_{l,s,\sigma}^{\dagger}c_{l,s,\sigma}\\ &= 2\eta\sum_{l,s}\mathbf{u}_{l,s}^T\begin{pmatrix}0 & 1\\ -1 & 0\end{pmatrix}\mathbf{p}_{l,s}\sigma c_{l,s,\sigma}^{\dagger}c_{l,s,\sigma}.\end{aligned} \tag{A4}$$

Substituting Eqs. (A1)–(A3) into Eq. (A4) and taking the transpose, we obtain

$$H_{e-cp} = -\frac{\sqrt{2}\eta}{N}\sum_{\mathbf{q},\mathbf{q}',\nu,\nu',s}g_{\mathbf{q},\mathbf{q}',s}^{\nu,\nu'}A_{\mathbf{q}}^{\nu}B_{-(\mathbf{q}-\mathbf{q}')}^{\nu'}S_{\mathbf{q}'}^{zss}, \tag{A5}$$

which is the same as Eq. (2).

APPENDIX B: THE EFFECTIVE HAMILTONIAN

As the expanded form of Eq. (A5) is

$$\begin{aligned}H_{e-cp} = \frac{-\sqrt{2}\eta}{N}\sum_{\nu\nu'qq's}g_{qq's}^{\nu\nu'}\big[\big(-a_q^{\nu}a_{q-q'}^{\nu'\dagger}+a_{-q}^{\nu\dagger}a_{-(q-q')}^{\nu'}\big)\\ +\big(-a_{-q}^{\nu\dagger}a_{q-q'}^{\nu'\dagger}+a_q^{\nu}a_{q'-q}^{\nu'}\big)\big]S_{q'}^{zss},\end{aligned} \tag{B1}$$

we can divide the E-CP interaction Hamiltonian into two parts,

$$H_{e-cp} = H_{e-cp-1}+H_{e-cp-2}, \tag{B2}$$

where

$$\begin{aligned}H_{e-cp-1} &= \frac{-\sqrt{2}\eta}{N}\sum_{\nu\nu'qq's}g_{qq's}^{\nu\nu'}\big(-a_q^{\nu}a_{q-q'}^{\nu'\dagger}+a_{-q}^{\nu\dagger}a_{-(q-q')}^{\nu'}\big)S_{q'}^{zss},\\ H_{e-cp-2} &= \frac{-\sqrt{2}\eta}{N}\sum_{\nu\nu'qq's}g_{qq's}^{\nu\nu'}\big(-a_{-q}^{\nu\dagger}a_{q-q'}^{\nu'\dagger}+a_q^{\nu}a_{q'-q}^{\nu'}\big)S_{q'}^{zss}.\end{aligned} \tag{B3}$$

Then, according to the two virtual phonon processes shown in the Feynman diagrams in Fig. 1(b), we can write the interaction matrix elements of electrons by exchanging two chiral phonons,

$$\sum_m \langle f|H_{e-cp}|m\rangle\langle m|H_{e-cp}|i\rangle/(E_i - E_m) = \sum_m \langle f|H_{e-cp-1}|m\rangle\langle m|H_{e-cp-1}|i\rangle/(E_i - E_m) + \sum_m \langle f|H_{e-cp-2}|m\rangle\langle m|H_{e-cp-2}|i\rangle/(E_i - E_m). \tag{B4}$$

Note that the initial state $|i\rangle$ and final state $|f\rangle$ is

$$|i\rangle = \left|n_{ks\sigma}, n_{k's'\sigma'}, n_{k'-q',s',\sigma'}, n_{k+q's\sigma}; N^{\nu}_{\pm q}, N^{\nu'}_{\pm(q-q')}\right\rangle, \tag{B5}$$

$$|f\rangle = \left|n_{ks\sigma} - 1, n_{k's'\sigma'} - 1, n_{k'-q',s',\sigma'} + 1, n_{k+q's\sigma} + 1; \quad N^{\nu}_{\pm q}, N^{\nu'}_{\pm(q-q')}\right\rangle, \tag{B6}$$

where n is the number of electrons, and N is the number of phonons.

Lastly, the total effective Hamiltonian can be written as

$$\begin{aligned}
H_{\text{eff}} &= H_{\text{eff}-1} + H_{\text{eff}-2} \\
&= -\frac{\eta^2}{N^2}\sum_{k,k',\sigma,\sigma',s,s'}\sum_{q,q',\nu,\nu'} \frac{2\sigma\sigma'\left(N^{\nu}_q - N^{\nu'}_{q-q'}\right)\left(\omega^{\nu}_q - \omega^{\nu'}_{q-q'}\right)}{\left(E_{ks\sigma} - E_{k+q's\sigma}\right)^2 - \left(\omega^{\nu}_q - \omega^{\nu'}_{q-q'}\right)^2} c^{\dagger}_{k+q's\sigma} c^{\dagger}_{k'-q's'\sigma'} c_{k's'\sigma'} c_{ks\sigma} \\
&\quad \times \left(g^{\nu,\nu'}_{q,q',s} g^{\nu',\nu}_{(q-q'),-q',s'} + g^{\nu,\nu'}_{-q,-q',s'} g^{\nu',\nu}_{-(q-q'),q',s} - g^{\nu,\nu'}_{q,q',s} g^{\nu,\nu'}_{-q,-q',s'} - g^{\nu',\nu}_{-(q-q'),q's} g^{\nu',\nu}_{(q-q'),-q',s'}\right) \\
&\quad - \frac{\eta^2}{N^2}\sum_{k,k',\sigma,\sigma',s,s'}\sum_{q,q',\nu,\nu'} \frac{2\sigma\sigma'\left(N^{\nu}_q + N^{\nu'}_{q-q'} + 1\right)\left(\omega^{\nu}_q + \omega^{\nu'}_{q-q'}\right)}{\left(E_{ks\sigma} - E_{k+q's\sigma}\right)^2 - \left(\omega^{\nu}_q + \omega^{\nu'}_{q-q'}\right)^2} c^{\dagger}_{k+q's\sigma} c^{\dagger}_{k'-q's'\sigma'} c_{k's'\sigma'} c_{ks\sigma} \\
&\quad \times \left(g^{\nu,\nu'}_{q,q',s} g^{\nu',\nu}_{(q-q'),-q',s'} + g^{\nu,\nu'}_{-q,-q',s'} g^{\nu',\nu}_{-(q-q'),q',s} + g^{\nu,\nu'}_{q,q',s} g^{\nu,\nu'}_{-q,-q',s'} + g^{\nu',\nu}_{-(q-q'),q',s} g^{\nu',\nu}_{(q-q'),-q',s'}\right).
\end{aligned} \tag{B7}$$

According to our numerical results, the E-CP interaction provides an effective repulsion for electrons, and the non-s-wave pairing symmetry could be attributed to this kind of repulsive interaction.

[1] V. Z. Kresin and S. A. Wolf, Rev. Mod. Phys. **81**, 481 (2009).

[2] A. Lanzara, P. V. Bogdanov, X. J. Zhou, S. A. Kellar, D. L. Feng, E. D. Lu, T. Yoshida, H. Eisaki, A. Fujimori, K. Kishio, J. I. Shimoyama, T. Noda, S. Uchida, Z. Hussain, and Z. X. Shen, Nature (London) **412**, 510 (2001).

[3] F. Giustino, M. L. Cohen, and S. G. Louie, Nature (London) **452**, 975 (2008).

[4] T. Egami, in *Symmetry and Heterogeneity in High Temperature Superconductors*, edited by A. Bianconi (Springer, Berlin, 2006), Chap. II.1, pp. 79–86.

[5] P. Baňacký, in *Symmetry and Heterogeneity in High Temperature Superconductors* (Ref. [4]), Chap. II.2, pp. 87–101.

[6] D. Reznik, L. Pintschovius, M. Ito, S. Iikubo, M. Sato, H. Goka, M. Fujita, K. Yamada, G. D. Gu, and J. M. Tranquada, Nature (London) **440**, 1170 (2006).

[7] Y. He, M. Hashimoto, D. Song, S.-D. Chen, J. He, I. M. Vishik, B. Moritz, D.-H. Lee, N. Nagaosa, J. Zaanen, T. P. Devereaux, Y. Yoshida, H. Eisaki, D. H. Lu, and Z.-X. Shen, Science **362**, 62 (2018).

[8] P. A. Lee, N. Nagaosa, and X. G. Wen, Rev. Mod. Phys. **78**, 17 (2006).

[9] A. G. McLellan, J. Phys. C: Solid State Phys. **21**, 1177 (1988).

[10] E. Anastassakis, E. Burstein, A. A. Maradudin, and R. Minnick, J. Phys. Chem. Solids **33**, 519 (1972).

[11] E. Anastassakis, E. Burstein, A. A. Maradudin, and R. Minnick, J. Phys. Chem. Solids **33**, 1091 (1972).

[12] E. Anastassakis and E. Burstein, J. Phys. C: Solid State Phys. **5**, 2468 (1972).

[13] L. Zhang and Q. Niu, Phys. Rev. Lett. **112**, 085503 (2014).

[14] L. Zhang and Q. Niu, Phys. Rev. Lett. **115**, 115502 (2015).

[15] Y. Ren, C. Xiao, D. Saparov, and Q. Niu, Phys. Rev. Lett. **127**, 186403 (2021).

[16] D. M. Juraschek, M. Fechner, A. V. Balatsky, and N. A. Spaldin, Phys. Rev. Mater. **1**, 014401 (2017).

[17] D. M. Juraschek and N. A. Spaldin, Phys. Rev. Mater. **3**, 064405 (2019).

[18] G. Xiong, H. Chen, D. Ma, and L. Zhang, Phys. Rev. B **106**, 144302 (2022).

[19] J. Zhong, H. Sun, Y. Pan, Z. Wang, X. Xu, L. Zhang, and J. Zhou, Phys. Rev. B **107**, 125147 (2023).

[20] R. M. Geilhufe and W. Hergert, Phys. Rev. B **107**, L020406 (2023).

[21] D. Saparov, B. Xiong, Y. Ren, and Q. Niu, Phys. Rev. B **105**, 064303 (2022).

[22] D. Yao and S. Murakami, Phys. Rev. B **105**, 184412 (2022).

[23] J. Bonini, S. Ren, D. Vanderbilt, M. Stengel, C. E. Dreyer, and S. Coh, Phys. Rev. Lett. **130**, 086701 (2023).

[24] H. Zhu, J. Yi, M. Li, J. Xiao, L. Zhang, C. Yang, R. A. Kaindl, L. Li, Y. Wang, and X. Zhang, Science **359**, 579 (2018).

[25] K. Kim, E. Vetter, L. Yan, C. Yang, Z. Wang, R. Sun, Y. Yang, A. Comstock, X. Li, J. Zhou, L. Zhang, W. You, D. Sun, and J. Liu, Nat. Mater. **22**, 322 (2023).

[26] F. G. G. Hernandez, A. Baydin, S. Chaudhary, F. Tay, I. Katayama, J. Takeda, H. Nojiri, A. K. Okazaki, P. H. O. Rappl, E. Abramof, M. Rodriguez-Vega, G. A. Fiete, and J. Kono, arXiv:2208.12235.

[27] S. R. Tauchert, M. Volkov, D. Ehberger, D. Kazenwadel, M. Evers, H. Langer, A. Donger, A. Book, W. Kreuzpaintner, U. Nowak, and P. Baum, Nature (London) **602**, 73 (2022).
[28] G. Schaack, J. Phys. C: Solid State Phys. **9**, L297 (1976).
[29] J. Holanda, D. S. Maior, A. Azevedo, and S. M. Rezende, Nat. Phys. **14**, 500 (2018).
[30] T. F. Nova, A. Cartella, A. Cantaluppi, M. Först, D. Bossini, R. V. Mikhaylovskiy, A. V. Kimel, R. Merlin, and A. Cavalleri, Nat. Phys. **13**, 132 (2017).
[31] B. Cheng, T. Schumann, Y. Wang, X. Zhang, D. Barbalas, S. Stemmer, and N. P. Armitage, Nano Lett. **20**, 5991 (2020).
[32] K. Ishito, H. Mao, Y. Kousaka, Y. Togawa, S. Iwasaki, T. Zhang, S. Murakami, J. Kishine, and T. Satoh, Nat. Phys. **19**, 35 (2023).
[33] W. J. Choi, K. Yano, M. Cha, F. M. Colombari, J. Kim, Y. Wang, S. H. Lee, K. Sun, J. M. Kruger, A. F. de Moura, and N. A. Kotov, Nat. Photonics **16**, 366 (2022).
[34] G. Grissonnanche, S. Thériault, A. Gourgout, M. E. Boulanger, E. Lefrancois, A. Ataei, F. Laliberté, M. Dion, J. S. Zhou, S. Pyon, T. Takayama, H. Takagi, N. Doiron-Leyraud, and L. Taillefer, Nat. Phys. **16**, 1108 (2020).
[35] C. Stamm, T. Kachel, N. Pontius, R. Mitzner, T. Quast, K. Holldack, S. Khan, C. Lupulescu, E. F. Aziz, M. Wietstruk, H. A. Dürr, and W. Eberhardt, Nat. Mater. **6**, 740 (2007).
[36] M. Hamada, E. Minamitani, M. Hirayama, and S. Murakami, Phys. Rev. Lett. **121**, 175301 (2018).
[37] M. Hamada and S. Murakami, Phys. Rev. Res. **2**, 023275 (2020).
[38] J. Medina Dueñas, H. L. Calvo, and L. E. F. Foa Torres, Phys. Rev. Lett. **128**, 066801 (2022).
[39] T. Takimoto, T. Hotta, and K. Ueda, Phys. Rev. B **69**, 104504 (2004).
[40] R. Shankar, *Principles of Quantum Mechanics*, 2nd ed. (Plenum, New York, 1994), p. 468.
[41] B. Stritzker and W. Buckel, Z. Phys. **257**, 1 (1972).
[42] H. J. Bornemann, D. E. Morris, and H. B. Liu, Physica C: Superconductivity **182**, 132 (1991).
[43] A. M. Schaeffer, S. R. Temple, J. K. Bishop, and S. Deemyad, Proc. Natl. Acad. Sci. USA **112**, 60 (2015).
[44] A. Stucky, G. W. Scheerer, Z. Ren, D. Jaccard, J.-M. Poumirol, C. Barreteau, E. Giannini, and D. van der Marel, Sci. Rep. **6**, 37582 (2016).
[45] D. J. Pringle, G. V. M. Williams, and J. L. Tallon, Phys. Rev. B **62**, 12527 (2000).